Society of Medical Education & Research

2023, Volume 3, Issue 2, Page No: 120-140

ISSN: 3108-4834

Archive of International Journal of Cancer and Allied Science

Targeting CDCP1 to Amplify CD8⁺ T cell Cytotoxicity via JAK/STAT Signaling in Cervical Cancer

Juan Carlos Ramirez[1], Diego Armando Lopez[1]

[1]Department of Oncology, Fundación Santa Fe de Bogotá, Bogotá, Colombia.

***E-mail** ✉ j.ramirez.fsfb@yahoo.com

Abstract

Cervical cancer continues to pose a significant global health burden. Discovering novel targets for immunotherapy could offer a valuable strategy to improve treatment outcomes. This research investigates how CUB domain-containing protein 1 (CDCP1) influences cervical cancer development and examines its promise as a target for therapy. We carried out in-depth investigations using clinical patient datasets and animal-based preclinical models to explore the link between CDCP1 levels and outcomes in cervical cancer. In parallel, we used both immunodeficient and immunocompetent mouse models to examine how CDCP1 shapes the tumor immune landscape, particularly its influence on infiltrating T lymphocytes—such as cytotoxic T cells (CTLs) and regulatory T cells (Tregs). Follow-up mechanistic experiments were conducted to uncover the signaling mechanisms behind CDCP1's role in immune regulation, highlighting its binding to the T-cell surface receptor CD6 and the resulting stimulation of the JAK-STAT pathway. Our findings indicate that elevated CDCP1 expression correlates with unfavorable prognosis and impaired T cell infiltration in cervical cancer patients. In particular, it disrupts the function of cytotoxic T lymphocytes (CTLs) and regulatory T cells (Tregs). At the mechanistic level, CDCP1 interacts directly with CD6 on T cells, leading to suppression of the JAK-STAT signaling pathway. Furthermore, the research shows that pharmacological inhibition of CDCP1 using 8-prenylnaringenin (8PN) significantly inhibits tumor progression in animal models while boosting antitumor immune responses. By shaping the tumor immune microenvironment, CDCP1 significantly contributes to the progression of cervical cancer. Interventions aimed at CDCP1 could represent an effective strategy to improve patient prognosis.

Keywords: Cervical cancer, Immunotherapy, Global health, Immunodeficient

Introduction

Cervical cancer remains a significant global health concern, ranking fourth in both incidence and mortality among gynecologic malignancies [1, 2]. In 2022, approximately 604,000 new cases and 342,000 deaths were reported worldwide [3]. Standard treatment approaches include surgery, radiotherapy, and chemotherapy [4, 5]; however, patients with recurrent or metastatic disease face a dismal prognosis, with a 5-year survival rate below 20% despite systemic therapy [6, 7]. The limited effectiveness of current treatments and the associated adverse effects highlight the urgent need for alternative therapeutic strategies. Immunotherapy, which seeks to harness and modulate the host immune system for more precise targeting of cancer cells, has emerged as a promising avenue for cervical cancer treatment. Immune checkpoint inhibitors directed against PD-1, PD-L1, and CTLA-4 have demonstrated clinical efficacy in various cancers [8, 9], yet response rates to pembrolizumab in cervical cancer remain modest at around 15% [10]. These findings underscore the necessity of deepening our understanding of the cervical cancer immune microenvironment and identifying novel molecular targets for therapy.

HPV infection is a key driver of cervical cancer. During infection, the virus evades immune detection and

Access this article online https://smerpub.com/

Received: 14 May 2023; **Accepted:** 27 September 2023

How to cite this article: Ramirez JC, Lopez DA. Targeting CDCP1 to Amplify CD8⁺ T cell Cytotoxicity via JAK/STAT Signaling in Cervical Cancer. Arch Int J Cancer Allied Sci. 2023;3(2):xx-xx. https://doi.org/10.51847/DogwvQxwbw

establishes an immunosuppressive tumor microenvironment by releasing cytokines, which hinders the recruitment of antitumor immune cells and weakens immune surveillance [11, 12]. Prior work suggests that ideal immunotherapy targets should satisfy three criteria: selectively counteracting tumor-specific immune evasion [13, 14], regulating immune activity within the tumor microenvironment [15], and reprogramming antitumor immunity locally [16, 17]. Evidence increasingly points to local immune dysfunction, rather than systemic immune suppression, as a major contributor to cervical cancer pathogenesis [18]. Consequently, a comprehensive characterization of the tumor immune microenvironment is critical for discovering viable immunotherapeutic targets. Using single-cell sequencing, Li and Hua [19] identified a profoundly immunosuppressive state in cervical cancer tissues, characterized by extensive infiltration of exhausted CD8+ T cells. These observations align with findings from Gu *et al*.[20] and studies in other cancers, including lung and liver[21, 22] CD8+ T cells are central to regulating antitumor immunity [23], and effector T cells play a particularly crucial role in shaping the cervical cancer immune landscape. Therefore, molecules that influence T cell function represent promising targets for reprogramming the tumor microenvironment and enhancing antitumor immune responses [9, 24].

CUB domain-containing protein 1 (CDCP1), also referred to as CD318, SIMA135, or TRASK, was initially identified by Scherl-Mostageer *et al*. in 2001 as overexpressed in colorectal cancer [25]. Subsequent studies have shown that CDCP1 is highly expressed across multiple tumor types, including prostate [26, 27], breast [28], lung [29, 30], ovarian [31], bladder [32], and pancreatic cancers [33, 34], and its expression correlates with metastasis, recurrence, poor prognosis, and therapy response. Mechanistically, CDCP1 regulates intracellular signaling pathways that drive tumor cell survival, proliferation, metastasis, and resistance to treatment. For example, it can interact with Src to reduce cell adhesion and facilitate metastasis [35], directly associate with EGFR or Her2 to amplify oncogenic signaling and induce drug resistance [36], and, in Ras-mutant tumors, activate the Ras/ERK pathway to increase MMP2 activation and MMP9 secretion, promoting extracellular matrix degradation and tumor invasion [37]. While preliminary evidence suggests a role for CDCP1 in cervical cancer [38, 39], its exact function, particularly in modulating the tumor immune microenvironment, has not been fully elucidated. Understanding these mechanisms is therefore essential for developing new therapeutic strategies aimed at improving outcomes for patients with cervical cancer.

In this study, we aim to investigate the contribution of CDCP1 to cervical cancer progression and assess its potential as a therapeutic target. We will examine CDCP1 expression in cervical cancer tissues and evaluate correlations with clinical outcomes to determine its prognostic significance. Using both in vitro and in vivo models, we will explore how CDCP1 influences tumor growth and modulates the tumor immune microenvironment, with a focus on tumor-infiltrating T cells. By delineating the biological roles, molecular mechanisms, and immune interactions of CDCP1, we aim to provide insights into novel therapeutic strategies for cervical cancer management.

Materials and Methods

Clinical specimens

Between January 2012 and December 2020, 206 paraffin-embedded cervical cancer specimens were collected from patients who underwent radical hysterectomy. None of these patients had received preoperative radiotherapy or chemotherapy, and complete pathological data were available for all cases. For comparison, cervical tissues from 30 patients undergoing hysterectomy for benign gynecological conditions were included as controls.

TCGA data analysis

mRNA sequencing data from 306 cervical cancer cases were obtained from the TCGA database. Gene expression levels were normalized, and cytotoxic T lymphocyte (CTL) scores were calculated for each patient by averaging expression of key CTL markers: CD8A, CD8B, GZMA, GZMB, and PRF1 [40]. Patients were stratified into high- and low-CTL score groups according to whether their CTL score was above or below the cohort mean. Differential gene expression analysis between the two groups was conducted using edgeR, with thresholds set at $|\log2FC| > 2$ and $p < 0.01$. Overall survival and disease-free survival were analyzed using the median CTL score as the cut-off. Heatmaps were generated to visualize CDCP1 expression alongside CTL-associated gene patterns.

Cell culture

Human cervical cancer SiHa cells and mouse cervical cancer U14 cells were obtained from the Shanghai Institute of Life Sciences (Chinese Academy of Sciences). Human T cells were isolated from peripheral blood of healthy donors, and mouse T cells were harvested from C57 mouse spleens. Tumor cells were cultured in DMEM (Gibco) supplemented with 10% fetal bovine serum, L-glutamine, penicillin, and streptomycin. T cells were maintained in serum-free x-VIVO 15 medium supplemented with 200 U/mL IL-2. All cultures were incubated at 37°C in a humidified atmosphere containing 5% CO2.

Cell transfection

U14 cells were transiently transfected with siRNA (CRN1023, Cohexion) using Lipofectamine (Thermo Fisher, USA). Stable knockdown and overexpression of CDCP1 in U14 and SiHa cells were achieved using lentiviral vectors carrying shRNA or CDCP1 expression plasmids. Target sequences were as follows:

ShRNA-Murine Forward (F): CCGGCCATCAAGTATGCAGTGAATTCTCGAGAATTCACTGCATACTTGATGGTTTTTG

ShRNA-Murine Reverse (R): AATTCAAAAACCATCAAGTATGCAGTGAATTCTCGAGAATTCACTGCATACTTGATGG

ShRNA-Human Forward (F): CCGGCCTCAACTTCAATGTCTCCAACTCGAGTTGGAGACATTGAAGTTGAGGTTTTTG

ShRNA-Human Reverse (R): AATTCAAAAACCTCAACTTCAATGTCTCCAACTCGAGTTGGAGACATTGAAGTTGAGG

Plasmids used included pLKO.1-Puro (P0258), pSIN-EF2-Puro (P40791), and pSIN-EF1a-Cdcp1 (mouse)-Puro (P50225) from MiaoLing Biology, China. Lentiviral packaging was performed in 293T cells, and fresh virus-containing supernatants were used to infect target cells. Following infection, puromycin selection (4 μg/mL for U14, 2 μg/mL for SiHa) was applied to establish stable CDCP1 knockdown, overexpression, and control cell lines.

RNA extraction and qPCR

RNA was extracted using the RNA-Quick Purification Kit (RN001, ES Science) according to the manufacturer's instructions. Concentrations were determined with a NanoDrop 2000, and cDNA synthesis was performed using the Reverse Transcription Kit (R223-01, Vazyme). RT-qPCR was carried out with AG11701 qPCR reagent (Accurate Biology). Primer sequences were as follows:

CDCP1-Human Forward (F): CTGAACTGCGGGGTCTCTATC

CDCP1-Human Reverse (R): GTCCCCAGCTTTATGAGAACTG

CDCP1-Murine Forward (F): GAGCTACCCATCCTCAACAGA

CDCP1-Murine Reverse (R): GTCGAGGGGTTGCGAACTG

IFN-γ-Murine Forward (F): CAGCAACAGCAAGGCGAAAAAGG

IFN-γ-Murine Reverse (R): TTTCCGCTTCCTGAGGCTGGAT

IFNγR1-Murine Forward (F): CTTGAACCCTGTCGTATGCTGG

IFNγR1-Murine Reverse (R): TTGGTGCAGGAATCAGTCCAGG

IL2-Murine Forward (F): GCGGCATGTTCTGGATTTGACTC

IL2-Murine Reverse (R): CCACCACAGTTGCTGACTCATC

IL6-Murine Forward (F): TACCACTTCACAAGTCGGAGGC

IL6-Murine Reverse (R): CTGCAAGTGCATCATCGTTGTTC

IL10-Murine Forward (F): CGGGAAGACAATAACTGCACCC

IL10-Murine Reverse (R): CGGTTAGCAGTATGTTGTCCAGC

ACTB-Murine Forward (F): GTGACGTTGACATCCGTAAAGA

ACTB-Murine Reverse (R): GCCGGACTCATCGTACTCC

ACTB-Human Forward (F): CATGTACGTTGCTATCCAGGC

ACTB-Human Reverse (R): CTCCTTAATGTCACGCACGAT

Immunoprecipitation

Cell lysates were incubated with 4 μg anti-CD6 antibody for 1 hour at room temperature. Protein A-Agarose (50 μL) was added for an additional hour, and immunocomplexes were eluted in 20 μL buffer for downstream immunoblotting.

Western blot

Cells were lysed in 1× SDS sample buffer (Beyotime), proteins separated on 10% SDS-PAGE gels, and

transferred to 0.45 µm PVDF membranes. Membranes were blocked with 5% skim milk in PBST for 60 min at room temperature, then incubated overnight at 4°C with primary antibodies: CDCP1 antibodies: ab1377 (Abcam) and YT5291 (Immunoway), JAK1 antibody: #3332S (CST), Phospho-JAK1 (Tyr1034/1035): #3331 (CST) , STAT1 antibody: AF6300 (Affinity) , Phospho-STAT1 (Tyr701): AF3300 (Affinity) , STAT3 antibody: AF6294 (Affinity) , Phospho-STAT3 (Tyr705): AF3293 (Affinity) , Beta-actin antibody: 66009-1 (Proteintech). After washing, membranes were incubated with secondary antibodies for 1 hour at room temperature and visualized using enhanced chemiluminescence. Band intensities were quantified using ImageJ.

Immunohistochemistry

Paraffin sections (5 µm) were deparaffinized, rehydrated, and antigen retrieval performed under high-temperature, high-pressure conditions with alkaline EDTA. Sections were blocked with goat serum and incubated overnight at 4°C with primary antibodies: anti-CDCP1 (ab1377, Abcam), anti-CD8 (ZA-0508, ZSGB-BIO), or anti-CD3 (ZA-0503, ZSGB-BIO). HRP-conjugated secondary antibodies were applied for 1 hour at room temperature, followed by DAB staining and hematoxylin counterstaining. Slides were dehydrated, mounted, and scored by two pathologists. Staining was assessed as the product of area (0=0%, 1=<25%, 2=25–50%, 3=50–75%, 4=>75%) and intensity (0=none, 1=weak, 2=moderate, 3=strong). Patients were grouped into high- or low-staining categories based on a median score of 6.

Immunofluorescence

Five-micrometer paraffin sections were deparaffinized, rehydrated, and subjected to antigen retrieval with alkaline EDTA. Sections were blocked with 5% BSA and incubated overnight at 4°C with primary antibodies (anti-CDCP1, anti-CD8). After washing, fluorophore-conjugated secondary antibodies (AF488, AF555, Thermo) were applied for 1 hour at room temperature in the dark. Nuclei were stained with DAPI, and slides were mounted in anti-fade medium. Fluorescence intensity was used to assess staining.

Cell immunofluorescence labeling

SiHa cells were seeded in confocal dishes and incubated with 1 µg/mL recombinant human CD6-Fc fusion protein (17051-H02H-100, Sino Biological) or IgG-Fc control for 4 hours at 37°C [41]. Cells were then fixed and permeabilized with 100% methanol for 15 min at −20°C, blocked with PBS containing 10% donkey serum, 0.3% Triton X-100, and 1% BSA for 1 hour, and incubated overnight at 4°C with primary antibodies (anti-CDCP1, Alexa Fluor 488 donkey anti-human IgG, K0001D-AF488, Solarbio). After washing, secondary antibodies (Alexa Fluor 555 donkey anti-rabbit) were applied for 2 hours. Nuclei were counterstained with DAPI, and imaging was performed using an inverted fluorescence microscope (LSM780, Zeiss).

Cell proliferation assay

U14 cells with transient CDCP1 knockdown or overexpression, alongside their corresponding controls, were seeded into 96-well plates at 5000 cells per well and cultured at 37°C in a 5% CO_2 atmosphere. Cell viability was assessed daily over five consecutive days using the CCK-8 kit (GK10001, GLPBIO). For stable CDCP1-modified U14 cells generated via lentiviral transduction, 2000 cells per well were plated in 6-well plates. After 14 days, colonies were fixed with 4% paraformaldehyde, stained with crystal violet, and quantified using ImageJ software to determine clone formation efficiency.

In vitro co-culture assay

Mouse T cells were isolated from C57 spleens, and human T cells were obtained from peripheral blood mononuclear cells (PBMCs) using magnetic bead-based separation (EasySep Mouse Pan-Naïve T Cell Isolation Kit, 19848, STEMCELL Technologies; EasySep Direct Human T Cell Isolation Kit, 720305, 19661, STEMCELL Technologies). T cells were co-cultured with CDCP1 knockdown or overexpressing U14 and SiHa tumor cells at a 10:1 T cell-to-tumor cell ratio. In select experiments, T cells were pretreated for 6 hours with anti-CD6 antibody [42, 43] (10 µg/mL, MAB7271, R&D SYSTEMS), IgG control (BN20604, BIORIGIN), or 8PN (12.5 µM, I332693, Aladdin) prior to co-culture. Some co-cultures were supplemented with T cell activators, including Anti-Mouse CD3/CD28 SAFIRE purified antibodies (05112-25-500 and 10312-25-500, PeproTech) or ImmunoCult Human CD3/CD28 T Cell Activator (10971, STEMCELL Technologies), depending on experimental requirements. Tumor cell killing was evaluated via crystal violet staining, while T cell activity and functional changes were assessed by flow cytometry and Western blot. Additionally, T cells from select co-cultures were sorted for RNA sequencing

to explore transcriptional changes induced by tumor interaction.

Flow cytometry

Fluorescent antibodies were obtained from Biolegend. Human samples were stained with PerCP/Cy5.5 anti-CD3, FITC anti-CD4, Pacific Blue anti-CD8, APC anti-CD137, and PE anti-CD107a. Mouse samples included APC/FIRE750 anti-CD45.2, PerCP5.5 anti-F4/80, APC anti-CD11b, BV650 anti-CD11C, FITC anti-GR1, BV421 anti-Ly6G, PE anti-Ly6C, FITC anti-CD3, AF700 anti-CD4, BV650 anti-CD8, PE anti-CD25, AF647 anti-Foxp3, BV605 anti-IFNγ, and PC7 anti-GZMB. Tumors were enzymatically dissociated to single-cell suspensions, blocked with Mouse BD Fc Block at 4°C, and dead cells excluded using Zombie Aqua viability dye (Biolegend). Surface staining was performed for 30 minutes at 4°C. Intracellular cytokine staining was conducted after stimulating cells with 50 ng/mL PMA and 500 ng/mL ionomycin in the presence of brefeldin A for 4 hours, followed by fixation, permeabilization, and staining. Data were acquired on a Cytek Aurora cytometer and analyzed using FlowJo software.

Flow cytometry sorting

Live (Zombie Aqua-negative), CD3-positive T cells were sorted using a FACSAria cell sorter (BD Biosciences) and collected in RNAase-free tubes for downstream RNA sequencing and molecular analyses.

Animal studies

All animal procedures were approved by the Animal Ethics and Welfare Committee of Sun Yat-sen University. Female SPF-grade BALB/c nude mice and C57BL/6 mice (4–6 weeks old, 18–20 g) were obtained from Guangdong Medical Laboratory Animal Center and maintained under SPF conditions. For xenograft experiments, 1×10^6 U14 cells (CDCP1 knockdown, overexpressing, or control) were injected subcutaneously in 100 µL. Tumor growth was monitored every other day with caliper measurements, and volumes were calculated as $V = L \times W^2 / 2$. For in vivo interventions, mice with tumors of approximately 100 mm³ (day 10) were randomized to receive three weekly injections of 10 mg/kg anti-PD-1 (BE0146, BioXcell), anti-CD6, IgG isotype control (BE0083, BioXcell), or 8PN [42, 43] according to the experimental plan.[44]Humane endpoints were applied if tumor volume exceeded 1500 mm³ or at 30 days.

Statistical analysis

Data were analyzed using Prism V.9 (GraphPad Software). Associations between CDCP1 expression and clinicopathological features were assessed using χ^2 or Fisher's exact tests. Survival curves were generated with the Kaplan-Meier method and compared using the log-rank test. Quantitative results are reported as mean ± SEM, with comparisons made using two-tailed Student's t-tests. Statistical significance was defined as $p < 0.05$.

Results and Discussion

CDCP1 expression associates with poor prognosis and CTL modulation in cervical cancer

CTL scores in TCGA-CESC patients were calculated using CD8A, CD8B, GZMA, GZMB, and PRF1 expression [40]. Patients with higher CTL scores exhibited significantly improved overall survival compared to those with lower scores **(Figure 1a).** Membrane proteins potentially regulating immune infiltration were screened following the approach of Chen Leping *et al* [45]. Differential gene analysis identified five candidates—ITGAL, PTPRC, PTPRN, WAS, and CDCP1 **(Figure 1b)—**among which only CDCP1 expression significantly correlated with patient prognosis **(Figure 1a).** CDCP1, a membrane-associated gene, was enriched in patients with low CTL scores and likely contributes to the regulation of CTL function in cervical cancer **(Figure 1c).**

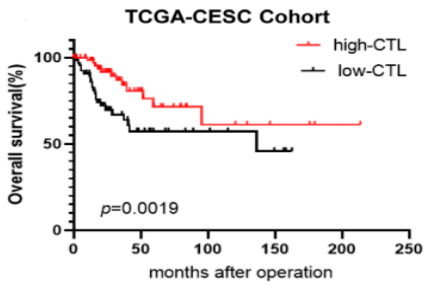

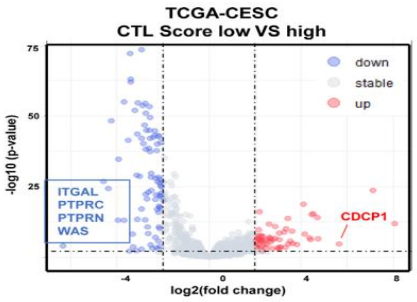

a)

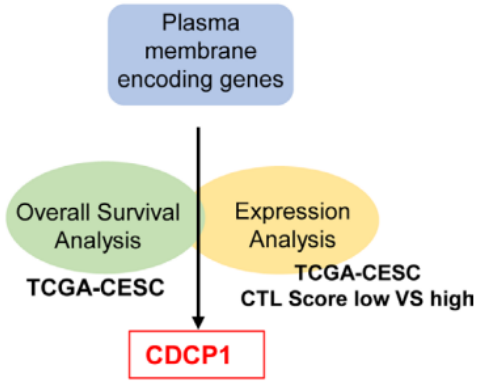
Plasma membrane encoding genes
Overall Survival Analysis
TCGA-CESC
Expression Analysis
TCGA-CESC
CTL Score low VS high
CDCP1

b)

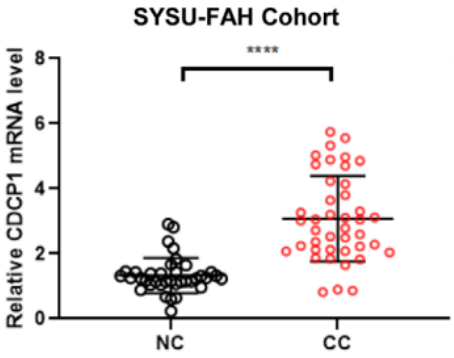
SYSU-FAH Cohort
****
Relative CDCP1 mRNA level
0
2
4
6
8
NC
CC

c)

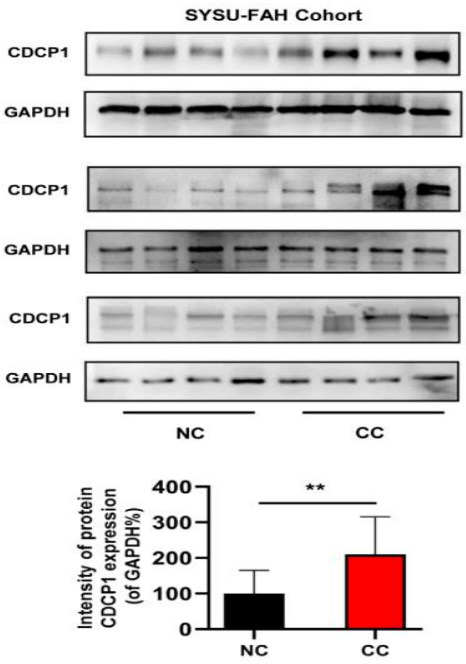
SYSU-FAH Cohort
CDCP1
GAPDH
CDCP1
GAPDH
CDCP1
GAPDH
NC
CC

d)

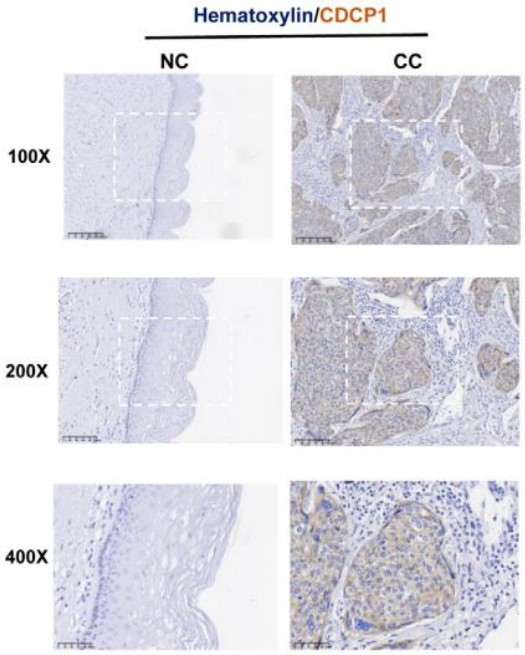
Hematoxylin/CDCP1
NC
CC
100X
200X
400X

e)

**
Intensity of protein CDCP1 expression (of GAPDH%)
0
100
200
300
400
NC
CC

f)

g)

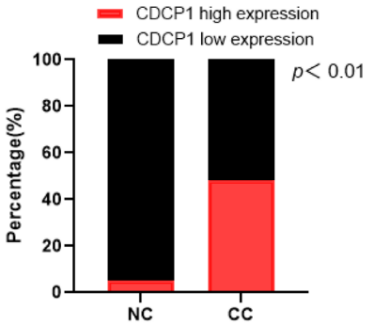
CDCP1 high expression
CDCP1 low expression
p< 0.01
Percentage(%)
0
20
40
60
80
100
NC
CC

h)

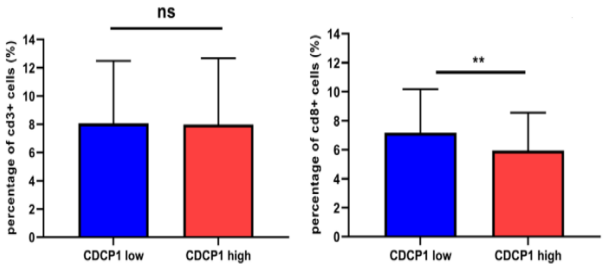
ns
percentage of cd3+ cells (%)
CDCP1 low
CDCP1 high
**
percentage of cd8+ cells (%)
CDCP1 low
CDCP1 high

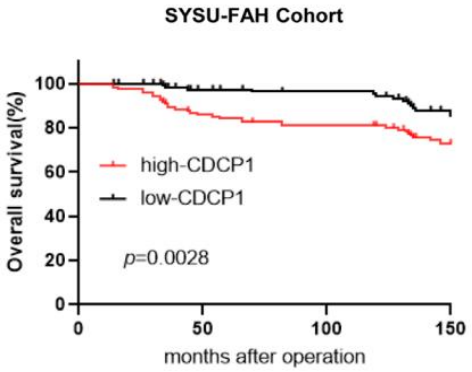

i)

Figure 1. CDCP1 expression associates with poor prognosis and modulates CTL activity in cervical cancer.

(a) Overall survival in TCGA-CESC patients stratified by cytotoxic T lymphocyte (CTL) scores, calculated from the average expression of CD8A, CD8B, GZMA, GZMB, and PRF1. The log-rank test was used to compare survival between patients with high versus low CDCP1 expression; $p<0.05$ was considered significant.

(b) Volcano plot highlighting genes differentially expressed between low-CTL and high-CTL groups. Genes significantly upregulated in the low-CTL group are shown in red, whereas downregulated genes are shown in blue. Membrane-associated genes of particular interest, including ITGAL, PTPRC, PTPRN, WAS, and CDCP1, are labeled. Thresholds for significance were set at $|\log2FC| > 2$ and $p<0.01$.

(c) Diagram summarizing the workflow used to identify membrane protein immunotherapy targets from the TCGA cervical cancer dataset. Differential gene expression and survival analysis identified membrane proteins correlated with poor prognosis and low CTL scores as potential targets.

(d) CDCP1 mRNA levels measured by qRT-PCR in patient samples.

(E) Western blot comparison of CDCP1 protein in normal cervical tissues (NC, n=12) and cervical cancer tissues (CC, n=12).

(f) Representative immunohistochemical staining for CDCP1 in NC and CC tissues at ×100, ×200, and ×400 magnifications. Scale bars = 200 μm, 100 μm, 50 μm.

(g) Percentage of samples with low versus high CDCP1 expression in NC (n=30) and CC (n=176) groups, quantified from IHC staining. Data are mean ± SEM; statistical significance was evaluated with Student's t-test: ns = not significant, **p<0.01, ****p<0.0001.

Results and Discussion

To explore the potential role of CDCP1 in cervical cancer, its expression was analyzed in a cohort of patients from the First Affiliated Hospital, Sun Yat-sen University. Both mRNA and protein levels of CDCP1 were markedly elevated in cancer tissues compared to normal cervix **(Figures 1d and e),** indicating that CDCP1 overexpression is a common feature of cervical cancer and may have prognostic relevance. IHC further confirmed stronger staining in tumor samples, and quantitative scoring showed a higher frequency of high-CDCP1 expression in cancer specimens **(Figures 1f and g).**

Next, we assessed the relationship between CDCP1 and tumor-infiltrating T cells by analyzing CD3+ and CD8+ populations in 153 cervical cancer tissues. No significant differences were observed for CD3+ T cell infiltration between high and low CDCP1 groups **(Figure 1h**, left). In contrast, tumors with elevated CDCP1 exhibited reduced CD8+ T cell infiltration **(Figure 1h**, right). Analysis of TCGA data supported these findings, revealing an inverse correlation between CDCP1 expression and CTL functional markers **(Figure 1b).**

Correlation analyses in 176 patients demonstrated that high CDCP1 levels were associated with adverse pathological features, including larger tumor size and pelvic lymph node metastasis **(Table 1).** Survival analysis confirmed that elevated CDCP1 predicted poorer overall survival **(Figure 1i).** Collectively, these results suggest that CDCP1 is not only a negative prognostic marker in cervical cancer but may also contribute to immune evasion, making it a potential target for therapeutic intervention.

Table 1. Association of CDCP1 expression with clinical and pathological characteristics in cervical cancer.

Clinicopathological Variable	Total (N=176)	Low CDCP1 Expression	High CDCP1 Expression	P Value
Age (years)				0.5296
≤42	67	33	34	
>42	109	59	50	
FIGO Stage				0.1083
Ia2	5	3	2	
Ib1	40	24	16	
Ib2	53	31	22	
Ib3	17	7	10	
IIa1	17	11	6	
IIa2	7	4	3	
IIB	3	2	1	
IIIC	34	10	24	
Tumor Size (cm)				0.02166
≤4	135	77	58	
>4	41	15	26	
Pathological Type				0.9438
Squamous cell carcinoma	152	79	73	
Adenocarcinoma	16	9	7	
Adenosquamous carcinoma	8	4	4	
Stromal Invasion				0.4302
<1/2	68	33	35	
≥1/2	108	59	49	
Lymphovascular Space Invasion (LVSI)				0.8416
Yes	24	13	11	
No	152	79	73	
Differentiation Grade				0.6464
Well	16	10	6	
Moderate	41	20	21	
Poor	119	62	57	
Pelvic Lymph Node Metastasis				0.002967
Yes	34	10	24	
No	142	82	60	
Vaginal Invasion				0.2268
Yes	27	17	10	
No	149	75	74	
Parametrial Infiltration				1
Yes	3	2	1	
No	173	90	83	
Recurrence				0.003017
Yes	14	2	12	
No	162	90	72	
Vital Status at Follow-Up				0.02198
Alive	160	88	72	
Dead	16	4	12	

Statistical analysis was performed using the Chi-squared test, with P-values below 0.05 considered significant and highlighted in bold.

CDCP1 modulates tumor growth in a manner dependent on the immune system

To assess the functional role of CDCP1 in tumor development, we generated U14 cells with either reduced

or elevated CDCP1 expression and implanted them into mouse models. Control cells, CDCP1-knockdown cells, and CDCP1-overexpressing cells were subcutaneously injected into 5-week-old female BALB/c-nu immunodeficient mice and 6-week-old female C57BL/6J immunocompetent mice, with four mice per experimental group (n=4). Representative images of tumor formation are shown in **Figures 2a and 2c**. Analysis of tumor growth demonstrated that silencing CDCP1 substantially suppressed tumor expansion in immunocompetent mice, while CDCP1 overexpression accelerated tumor growth compared to controls **(Figures 2b and 2d)**. These results indicate that CDCP1 promotes tumor progression in vivo, and its effects are dependent on the presence of a functional immune system.

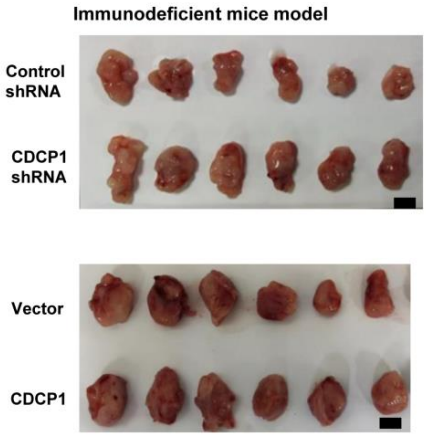

a)

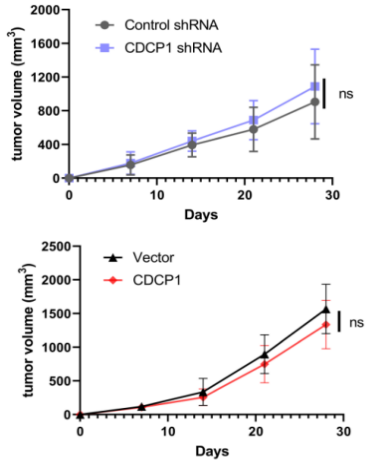

b)

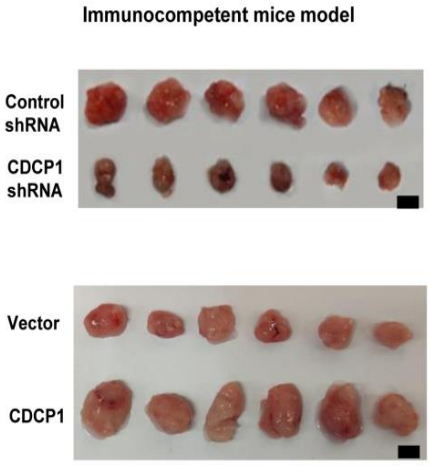

c)

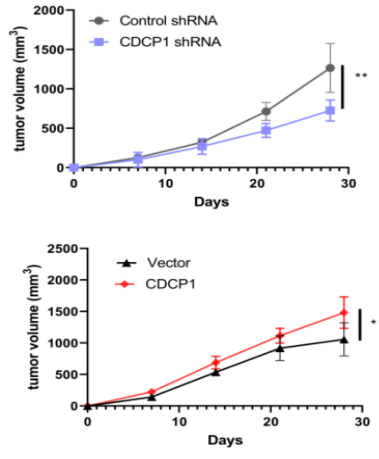

d)

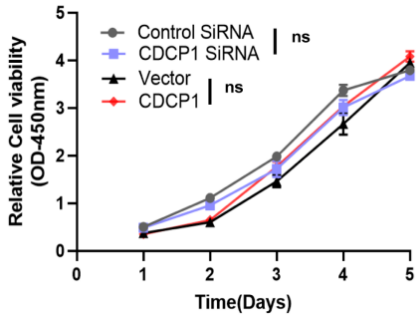

e)

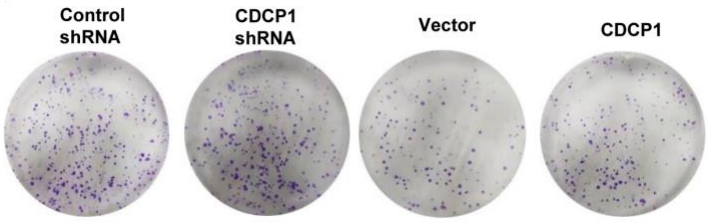

f)

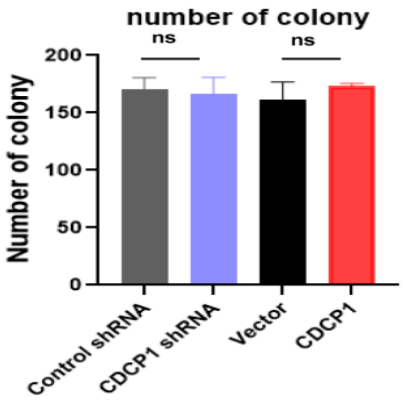

g)

Figure 2. CDCP1 regulates tumor growth through immune-dependent mechanisms.

(A, B) U14 cells with either normal, reduced, or elevated CDCP1 expression were injected subcutaneously into 5-week-old female BALB/c-nu immunodeficient mice (n=8 per group). Representative tumor images are displayed in panels A and B, with the growth kinetics plotted in the accompanying line graphs. Scale bar: 50 mm. Data are shown as mean ± SD; statistical significance is indicated by *p<0.05 and **p<0.01.

(C, D) The same experimental procedure was applied to 6-week-old female C57BL/6J immunocompetent mice (n=8 per group). Tumor images and growth curves are shown in panels C and D. Scale bar: 50 mm. Mean ± SD is presented, with ns representing non-significant differences; *p<0.05, **p<0.01.

(E–G) The proliferative behavior of U14 cells with control, knockdown, or overexpression of CDCP1 was evaluated using CCK-8 assays (E) and colony formation assays (F, G). All experiments were repeated at least three times. Data are presented as mean ± SEM and analyzed using one-way ANOVA (*p<0.05, **p<0.01).

To understand how CDCP1 influences tumor development, we assessed the intrinsic proliferation of U14 cells with altered CDCP1 expression. The CCK-8 assay results **(Figure 2e)** showed no significant changes in cell growth among the different groups. Similarly, long-term colony formation assays demonstrated that neither silencing nor overexpressing CDCP1 altered the capacity of U14 cells to form colonies **(Figures 2f and g).** These findings suggest that CDCP1 does not directly modulate tumor cell proliferation, indicating that its effects on tumor growth in vivo likely involve immune-mediated mechanisms.

Effect of CDCP1 expression on tumor-infiltrating immune cells in immunocompetent mice

To explore the impact of CDCP1 on the tumor immune microenvironment, U14 cells with varying levels of CDCP1 were injected into C57BL/6J mice. Tumors were collected on day 10 post-implantation and analyzed by flow cytometry.

The analysis **(Figure 3a)** revealed that total CD45+ leukocytes, CD11B+ myeloid cells, neutrophils, macrophages, CD3+ T cells, and CD4+ T cells did not differ significantly among the groups. Notably, CDCP1 knockdown tumors exhibited a substantial increase in CD8+ T cell infiltration, including elevated GZMB+IFNγ+ cytotoxic T lymphocytes, while CD25+FOXP3+ regulatory T cells were markedly decreased. In contrast, tumors with CDCP1 overexpression displayed reduced CD8+ T cell presence and an increase in Tregs. These observations indicate that CDCP1 modulates tumor progression predominantly by altering the composition and activity of tumor-infiltrating

T cells rather than by affecting overall immune cell numbers.

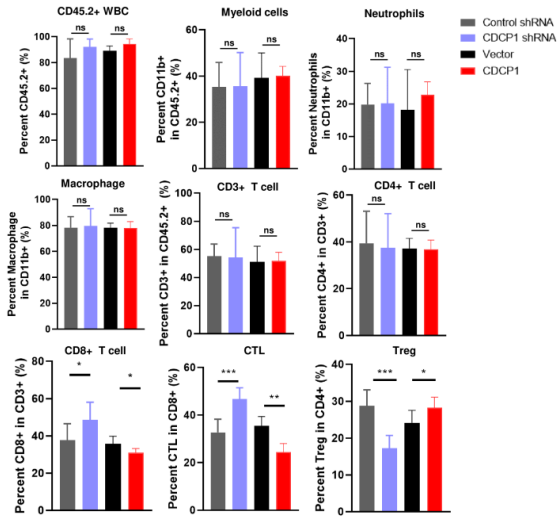

a)

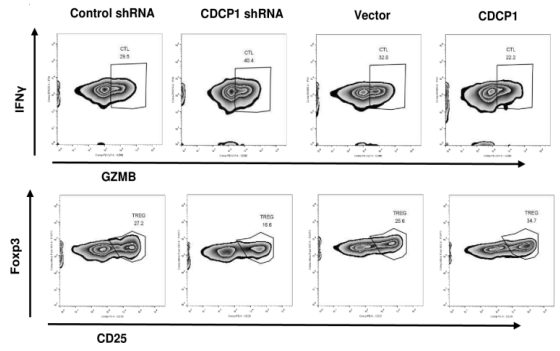

b)

Figure 3. Influence of CDCP1 expression on tumor-infiltrating immune cells in immunocompetent mouse models**.**

(A) Xenograft tumors were established using control, CDCP1 knockdown, and CDCP1-overexpressing U14 cells in immunocompetent mice. Harvested tumors were analyzed by flow cytometry to assess myeloid cells, neutrophils, macrophages (n=4), and T cells (n=4). Statistical comparisons between groups were performed using Student's t-test. Significance levels are indicated as *p<0.05, **p<0.01, ***p<0.001.

(B) Representative flow cytometry plots display the proportion of IFNγ+GZMB+ cytotoxic T lymphocytes (CTLs) and Foxp3+CD25+ regulatory T cells (Tregs) among the different groups. ns indicates non-significant differences.

To further investigate how CDCP1 influences T cell function, we established in vitro co-culture systems pairing murine and human tumor cell lines with T cells from the same species. This allowed us to determine whether altering CDCP1 expression in tumor cells directly affects T cell activity.

After 48 hours of co-culture with activated T cells at a tumor-to-T cell ratio of 1:10, the survival of murine U14 and human SiHa tumor cells was evaluated **(Figure 2a).** In both systems, knockdown of CDCP1 significantly reduced tumor cell survival under T cell-mediated cytotoxicity compared with control cells, whereas overexpression of CDCP1 enhanced tumor cell survival **(Figures 2b and c).**

We next assessed T cell activation within these co-cultures using flow cytometry. Murine T cells co-cultured with U14 cells at a 2.5:1 ratio for 16 hours exhibited the highest frequencies of IFNγ+ and GZMB+ cytotoxic T cells when paired with CDCP1 knockdown tumor cells, and the lowest frequencies with CDCP1-overexpressing cells **(Figure 2d).** Similarly, in the human co-culture system, CD8+ T cells expressing CD107a+CD137+ as well as IFNγ+ and GZMB+ CTLs were most abundant when cultured with CDCP1 knockdown tumor cells and significantly reduced with CDCP1-overexpressing tumor cells **(Figures 2e and f).** Overall, these findings indicate that CDCP1 on tumor cells shapes both the composition and functionality of tumor-infiltrating immune cells, enhancing antitumor responses through increased CTL activity and reduced Treg prevalence. This underscores the potential of targeting CDCP1 as a strategy to modulate the tumor immune microenvironment for cancer therapy.

CDCP1 inhibits T cell-mediated antitumor activity via CD6

CD6, a surface glycoprotein on T cells, is known to regulate T cell activation through ligand interactions.[46, 47] Recent studies have identified CDCP1—frequently upregulated in many cancers—as a second ligand for CD6.53 We hypothesized that in cervical cancer, CDCP1 modulates tumor-infiltrating T cell function primarily through CD6 engagement. To test this, we examined whether blocking CD6 could counteract CDCP1's effects on T cells.

Previous research has suggested that CD6 represents a promising immunotherapy target. Consistently, our results show that administering anti-CD6 monoclonal antibody to immunocompetent mice substantially

reduced tumor growth. Under anti-CD6 treatment, the impact of CDCP1 knockdown on tumor progression was no longer significant compared with controls **(Figures 4a and b),** indicating that CDCP1's regulation of T cell-mediated antitumor immunity is CD6-dependent.

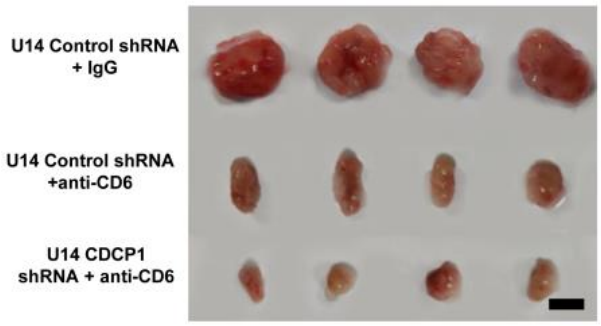

a)

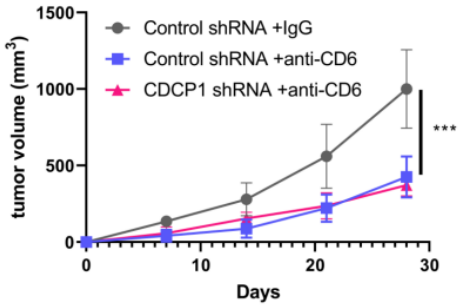

b)

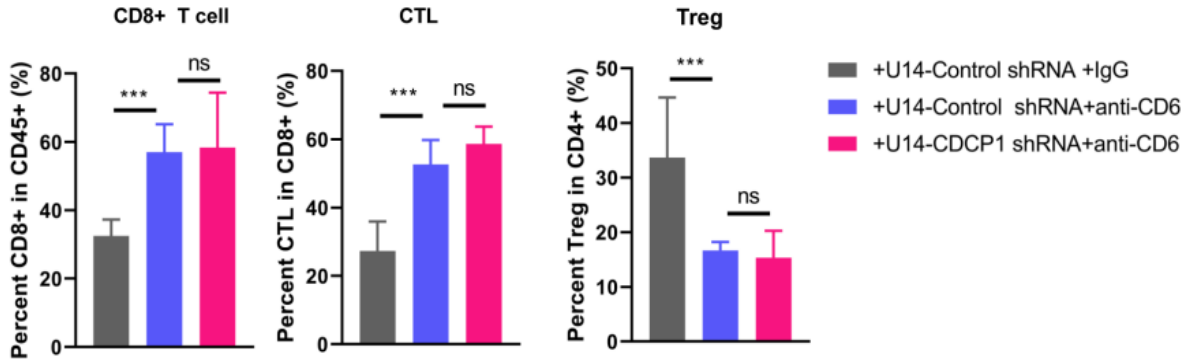

c)

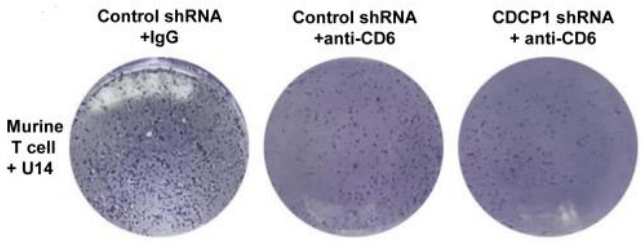

d)

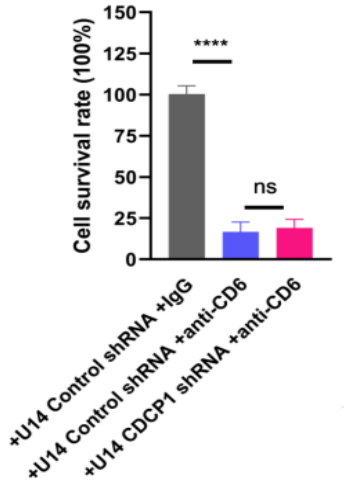

e)

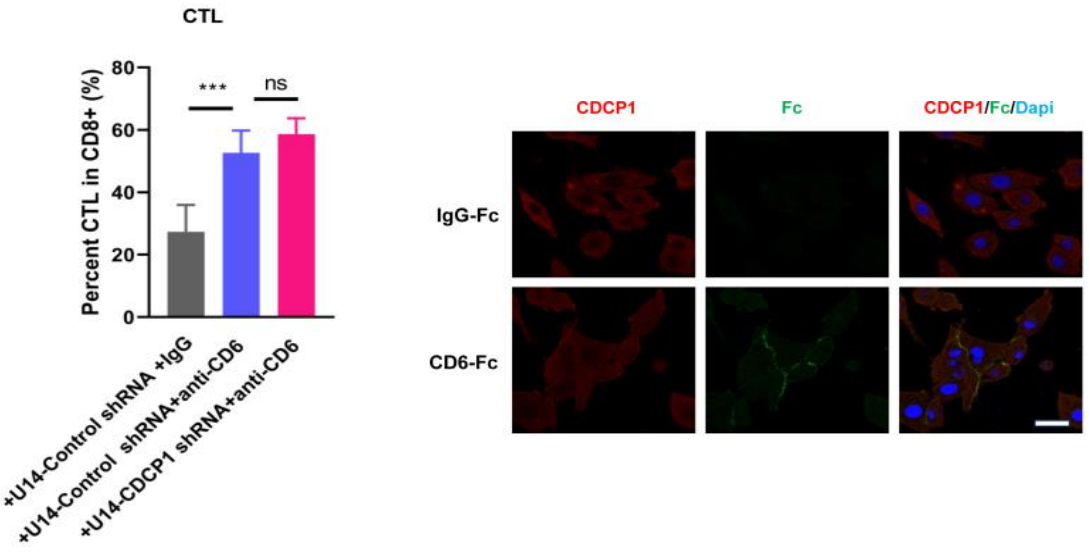

f) g)

Figure 4. CDCP1 suppresses T cell-mediated antitumor responses via CD6.

(A, B) Control and CDCP1 knockdown U14 cells were subcutaneously implanted into 6-week-old female C57BL/6J immunocompetent mice (n=4 per group). When tumors reached ~100 mm³, mice were randomly allocated to receive either intravenous anti-CD6 antibody or IgG control. Representative tumor images are shown in panel A (scale bar: 50 mm), and tumor volume progression over time is plotted in panel B. Data are expressed as mean ± SD. Statistical significance: *p<0.05, **p<0.01, ***p<0.001, ****p<0.0001.

(C) Tumor-infiltrating T cell populations were analyzed by flow cytometry, including CD8+ T cells, IFNγ+GZMB+ cytotoxic T lymphocytes (CTLs), and Foxp3+CD25+ regulatory T cells (Tregs). Mean ± SD values are presented. Student's t-test was used for comparisons between groups (*p<0.05, **p<0.01, ***p<0.001).

(D–F) In vitro, U14 cells with varying CDCP1 expression were co-cultured with activated T cells (tumor:T cell ratio = 1:2) for 48 hours in the presence of anti-CD6 antibody or IgG control. Crystal violet staining assessed tumor cell survival (panel E). T cell activation, including IFNγ+ and GZMB+ CTLs, was quantified (panel F). Values are mean ± SD; statistical comparisons were made using Student's t-test. ns = not significant, ***p<0.001.

(G) Immunofluorescence demonstrated binding between CDCP1 and exogenously added CD6 in SiHa human cervical cancer cells. CDCP1 (red) is normally distributed across the membrane and cytoplasm. Upon CD6-Fc treatment, co-localization was detected on the membrane (green signal). Scale bar: 5 µm.

Flow cytometry revealed that anti-CD6 treatment elevated CD8+ T cell infiltration in tumors, increased IFNγ+GZMB+ CTLs, and decreased Foxp3+CD25+ Tregs. Under CD6 blockade, the effects of CDCP1 knockdown on T cell functionality were abrogated **(Figure 4c).**

Co-culture experiments confirmed that inhibiting CD6 enhanced T cell-mediated tumor cell killing. Flow cytometric analysis showed increased activation of cytotoxic T cells. In this setting, CDCP1 knockdown had minimal additional effect, indicating that CDCP1 modulates T cell responses primarily through CD6 **(Figures 4d–f).**

CDCP1 binds CD6 and suppresses JAK-STAT signaling

Using immunofluorescence labeling,[41] CDCP1 was observed to interact with externally added CD6 in SiHa cells, consistent with prior studies identifying CDCP1 as a second ligand for CD6.[48] To investigate downstream signaling, RNA-seq was performed on T cells co-cultured with CDCP1-overexpressing or control U14 cells, both stimulated with anti-CD3/CD28 for 24 hours. KEGG pathway analysis revealed that immune-related pathways, including JAK-STAT signaling and cytokine-cytokine receptor interactions, were downregulated in T

cells exposed to CDCP1-overexpressing cells **(Figure 5a).**

Gene set enrichment analysis further highlighted suppression of the JAK-STAT pathway **(Figure 5b).** qRT-PCR confirmed that canonical JAK-STAT target genes, including Ifnγ, Ifngr1, and Il2, were decreased, whereas Il6 and Il10 were upregulated in T cells co-cultured with CDCP1-overexpressing U14 cells **(Figure 5c).**

Previous work shows that JAK-STAT signaling is critical for CTL differentiation and function. [49, 50] Inhibition of this pathway reduces cytotoxic molecule production, such as GZMB and IFNγ, thereby limiting T cell-mediated antitumor responses.

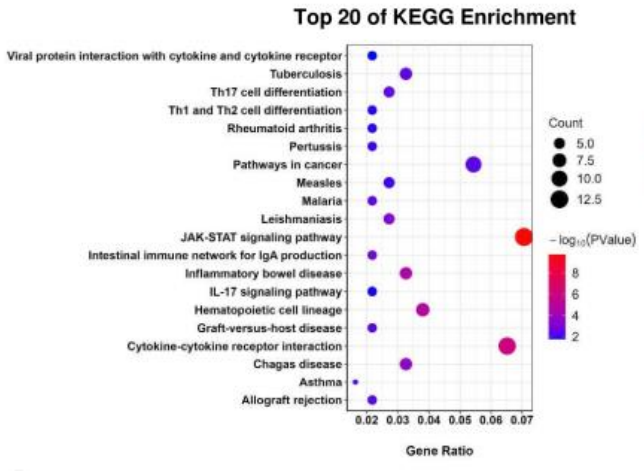

a)

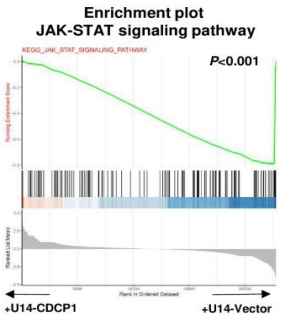

b)

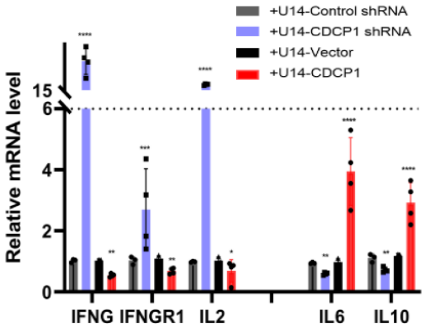

c)

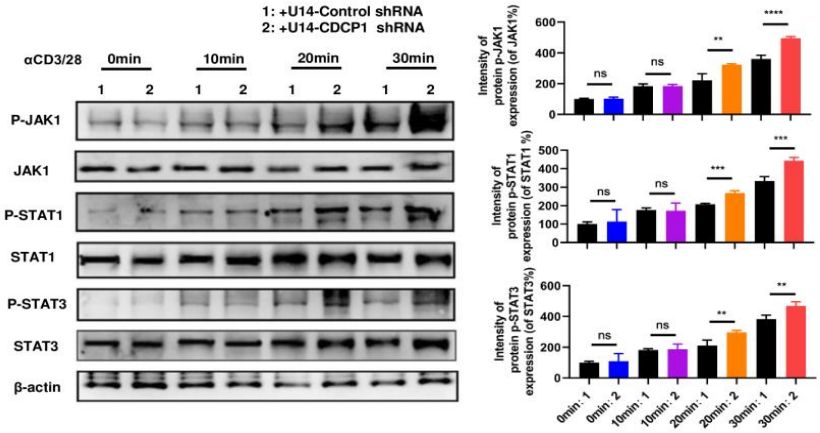

d)

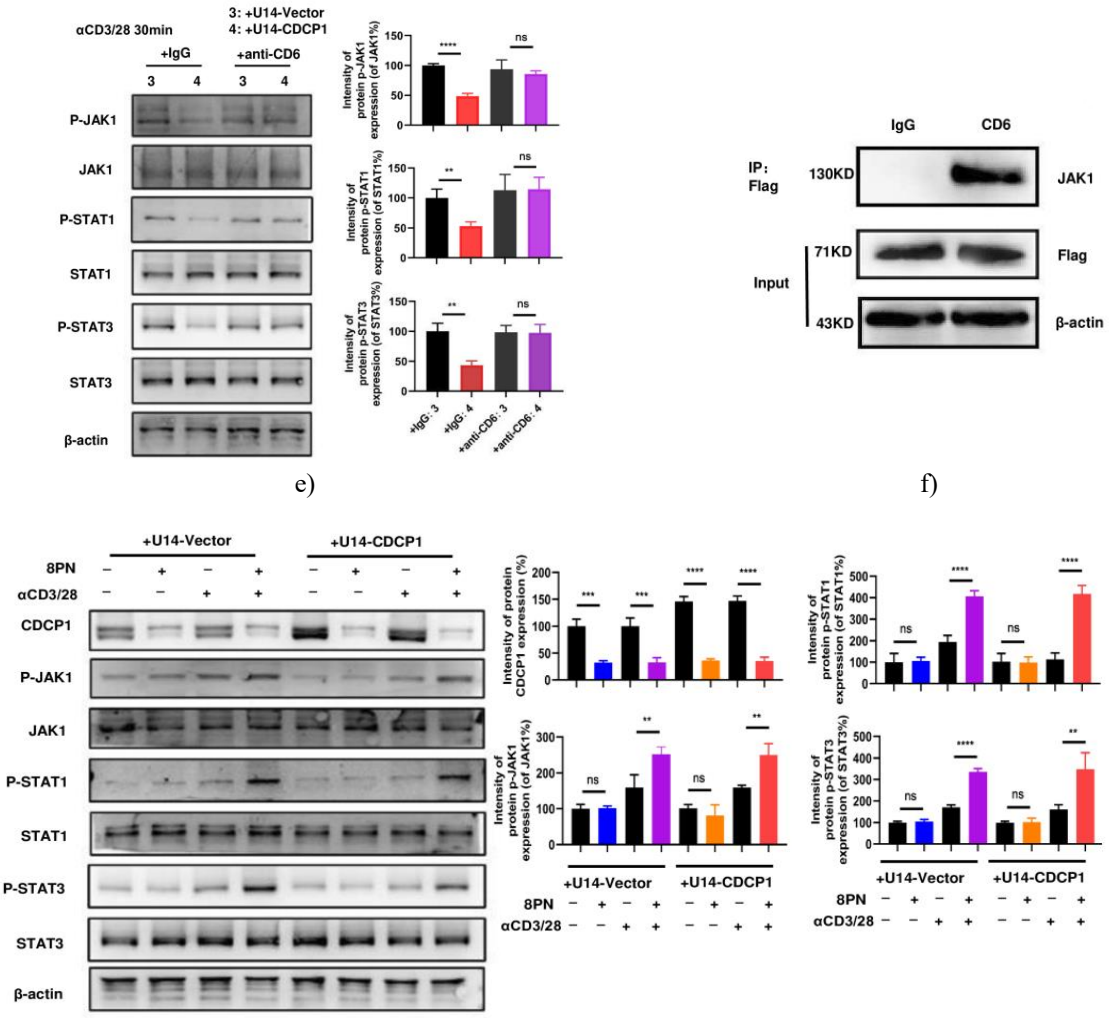

Figure 5. CDCP1 suppresses JAK-STAT signaling in T cells

(a) RNA-sequencing data from activated T cells co-cultured for 24 hours with CDCP1-overexpressing U14 cells versus control U14 cells were analyzed using KEGG to identify affected signaling pathways.

(b) Gene Set Enrichment Analysis (GSEA) revealed a pronounced downregulation of the JAK-STAT signaling pathway in T cells exposed to CDCP1-overexpressing tumor cells compared to controls ($p<0.001$).

(c) qRT-PCR validated changes in the expression of key JAK-STAT downstream genes in T cells co-cultured with U14 cells exhibiting varied CDCP1 expression.

(d) T cells co-cultured with control or CDCP1-silenced U14 cells were stimulated with anti-CD3 and anti-CD28 antibodies for 10–30 minutes. Phosphorylation of JAK1, STAT1, and STAT3 was assessed, showing elevated activation in CDCP1 knockdown conditions without changes in total protein levels.

(e) Similarly, T cells co-cultured with CDCP1-overexpressing U14 cells were evaluated in the presence or absence of anti-CD6 antibody, showing that CD6 blockade restored JAK-STAT phosphorylation.

(f) Immunoprecipitation using FLAG-tagged CD6 in CD8+ T cells from C57 mouse spleen confirmed an interaction between CD6 and JAK1. Lysates were immunoprecipitated with FLAG antibody and probed with anti-JAK1 and anti-FLAG.

(g) Pre-treatment of T cells co-cultured with CDCP1-overexpressing U14 cells with the inhibitor 8PN reactivated JAK1-STAT1/3 signaling. T cells were incubated with 8PN or DMSO for 24 hours, followed by pathway analysis. Significance was determined using

Student's t-test (*p<0.05, **p<0.01, ***p<0.001, ****p<0.0001; ns, not significant).

Suppression of JAK-STAT signaling influences cytokine production and receptor signaling, including IL2 and IL10, leading to enhanced recruitment and activation of immunosuppressive Tregs within the tumor microenvironment, ultimately dampening antitumor immune responses.

Analysis of T cells co-cultured with CDCP1 knockdown cells revealed increased phosphorylation of JAK1, STAT1, and STAT3 over time compared with control T cells, confirming that CDCP1 regulates the pathway via phosphorylation rather than total protein abundance **(Figure 5d).**

Since CDCP1 acts through CD6 on T cells, anti-CD6 antibody was used to block this interaction. In the presence of anti-CD6, overexpression of CDCP1 no longer inhibited phosphorylation of JAK1, STAT1, or STAT3 **(Figure 5e),** indicating that CD6 mediates CDCP1's effects on T cell signaling.

FLAG-tagged CD6 immunoprecipitation experiments confirmed its direct interaction with JAK1 inside T cells **(Figure 5f).**

Treatment with the CDCP1 inhibitor 8PN[43] effectively reduced CDCP1 expression in tumor cells and reactivated JAK1-STAT1/3 signaling in T cells [43]**(Figure 5g)**. These findings demonstrate that CDCP1 interferes with T cell-mediated antitumor immunity by binding CD6 and suppressing the JAK-STAT pathway.

Targeting CDCP1 as a therapeutic approach in cervical cancer

To assess the potential of CDCP1 inhibition as an immunotherapy strategy, we treated immunocompetent mice bearing subcutaneous cervical tumors with 8PN. Therapy began when tumors reached approximately 100 mm^3 (~day 10). 8PN treatment significantly reduced tumor growth and mass **(Figures 6a–c).** Furthermore, combining 8PN with anti-PD1 antibodies led to a synergistic enhancement in tumor suppression, indicating the potential of CDCP1-targeted therapy for improving antitumor immune responses.

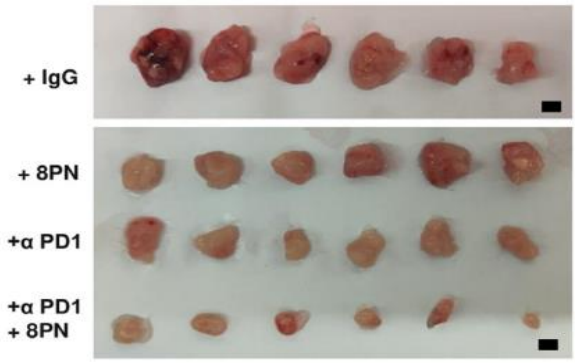

a)

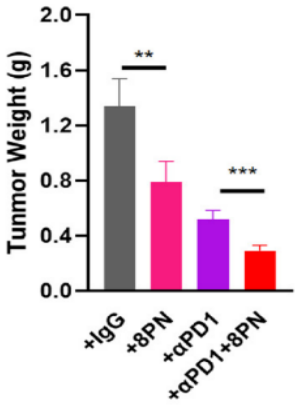

b)

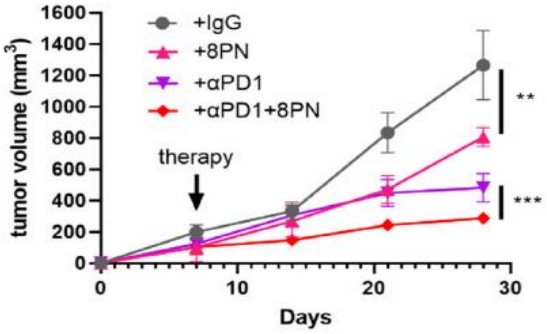

c)

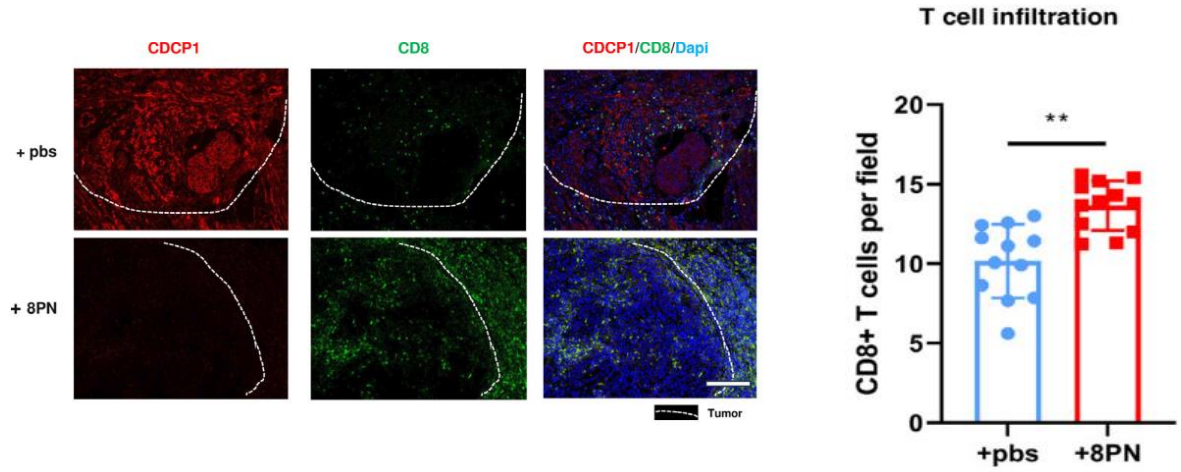

d) e)

Figure 6. CDCP1 inhibition restrains cervical cancer growth

U14 cervical cancer cells were implanted subcutaneously into 6-week-old female C57BL/6J mice. When tumors reached roughly 100 mm^3, mice were randomly assigned to receive intravenous treatments with either anti-CD6 antibody, anti-PD1 antibody, a combination of both, or IgG control. Representative images of the tumors are shown in panel A (scale bar: 50 mm). Panel B displays the excised tumors at 28 days post-inoculation. Tumor growth over time is illustrated in panel C. Values are presented as mean±SEM, with significance determined via Student's t-test (**p<0.01, ***p<0.001).

To evaluate the immune context of treated tumors, immunofluorescence staining for CD8+ T cells was performed. Representative images (panel D) highlight increased infiltration of CD8+ T cells in tumors from the 8PN-treated group, with the tumor boundary indicated by white dashed lines (scale bar: 50 μm). Quantitative analysis (panel E) confirmed a significant rise in CD8+ T cell density following CDCP1 inhibition (mean±SEM, *p<0.05, **p<0.01, ***p<0.001; ns = not significant).

These results suggest that pharmacological inhibition of CDCP1 with 8PN not only restricts tumor growth but also enhances the recruitment and activity of CD8+ cytotoxic T cells in the tumor microenvironment. Therefore, the antitumor effect observed is likely mediated by an immune-dependent mechanism, whereby suppression of CDCP1 potentiates T cell-mediated cytotoxicity.

Overall, this study provides compelling evidence that targeting CDCP1 could serve as an effective immunotherapeutic strategy to strengthen antitumor immunity and improve clinical outcomes in cervical cancer patients.

In this work, we explored the potential of CDCP1 as a target for immunotherapy in cervical cancer. Our analyses revealed that CDCP1 is overexpressed in tumor tissues and is linked to poor patient outcomes as well as reduced CTL infiltration, as observed in both the TCGA-CESC and FAH-SYSU cohorts. Using xenograft experiments in both immunodeficient and immunocompetent mice, we demonstrated that depletion of CDCP1 significantly impeded tumor growth in immunocompetent animals, emphasizing the contribution of immune cells in mediating CDCP1's tumor-promoting effects. Tumors with elevated CDCP1 expression exhibited lower CTL infiltration and higher levels of regulatory T cells (Tregs), whereas CDCP1-deficient tumors showed the opposite trend. Co-culture studies confirmed that CDCP1 expressed by tumor cells directly modulates T cell activity in the tumor microenvironment, affecting both their differentiation and effector function. This constitutes the first experimental evidence showing that CDCP1 directly interacts with T cells in cervical cancer.

We further investigated the mechanisms underlying CDCP1-mediated immune suppression. Both RNA-seq data and protein phosphorylation analyses **(Figure 5)** indicated that CDCP1 overexpression inhibits the JAK-STAT signaling pathway in co-cultured T cells, a central regulator of T cell activation that controls cytokine and growth factor expression. These findings uncover a novel pathway through which CDCP1 diminishes T cell function and facilitates tumor immune evasion.

CD6 is a type I transmembrane glycoprotein with a molecular weight of 105–130 kDa, belonging to the highly conserved scavenger receptor cysteine-rich superfamily. It is exclusively expressed on lymphocytes, including most mature T cells and approximately 50% of NK cells.[51, 52] CD6 has been implicated in T cell activation and immune regulation, though its function relative to the inhibitory CD5 receptor remains debated.[53, 54] CD6 participates in lymphocyte activation, proliferation, and survival through interactions with two known ligands: CD166/Activated Leukocyte Cell Adhesion Molecule (ALCAM)[55] and CD318, also known as CDCP1.[48]

ALCAM, part of the immunoglobulin superfamily, is expressed broadly in endothelial cells, epithelial cells, and APCs.[56] The CD6-ALCAM interaction contributes to T cell activation by stabilizing the immune synapse: CD6 colocalizes with the TCR/CD3 complex and binds ALCAM on APCs, prolonging T cell-APC interactions and optimizing cytotoxic T cell activation.[57] Costimulation of CD3 on PBMCs by ALCAM enhances T cell activation.

In contrast, our results reveal that CDCP1 binds CD6 and suppresses T cell activation, representing an inhibitory mechanism distinct from ALCAM. Despite both being CD6 ligands, their effects on T cells are opposite. This suggests that high CDCP1 expression on tumor cells may compete with ALCAM for CD6 binding, disrupting costimulatory signals required for CD3-mediated T cell activation, thereby promoting immune evasion. Experimental validation of this hypothesis remains necessary.

We evaluated the therapeutic effect of the CDCP1 inhibitor 8PN in cervical cancer models. Treatment with 8PN effectively reduced CDCP1 expression in vitro and in vivo **(Figures 5g and 6e),** confirming its inhibitory role. While 8PN targets CDCP1, potential off-target effects cannot be ruled out. As a phytoestrogen analog, previous studies reported that 8PN can influence breast cancer cell proliferation through estrogen receptor (ER) signaling.[58] In cervical cancer, ER expression is low in tumor cells and mostly localized to stromal fibroblasts rather than cancer cells,[59] suggesting minimal direct estrogenic effects of 8PN on tumor cells. Nevertheless, 8PN could modulate tumor progression indirectly via ER-positive fibroblasts in the tumor stroma.

Interestingly, in our mouse model, 8PN treatment increased CD8+ T cell infiltration into subcutaneous tumors **(Figures 6d–e),** indicating an enhancement of antitumor immune responses. Moreover, combination therapy with 8PN and anti-PD-1 antibody produced greater tumor suppression **(Figures 6a–c),** highlighting the potential therapeutic value of CDCP1-targeted strategies.

Conclusion

Overall, our findings suggest that CDCP1 acts as a negative regulator of T cell-mediated antitumor immunity and represents a promising target for immunotherapy in cervical cancer. These results provide new insights into the mechanisms of CDCP1-mediated immune evasion and support further preclinical and clinical investigation to optimize CDCP1-targeted treatments.

Acknowledgments: We thank the Pathology Department of the First Affiliated Hospital of Sun Yat-sen University for supporting the histological identification.

Conflict of Interest: None

Financial Support: The National Natural Science Foundation of China (82273365, 82072874 to SY, 82072884, 81872128 to JieL; 82303920 to QD; 82303390 to YC; 82403524 to CZ), National Key R&D Program of China (2022YFC2704201 to SY), Science and Technology Plan of Guangdong Province (2023A0505050102 to SY), Guangzhou Science and Technology Program (2024B03J1336 to SY), Xisike-Hengri Oncology Research Program (Y-HR2022MS-0730 to JieL), Technology Research Project of Zhongshan City (2022B3009 to YC and JunxiuL),Sun Yat-sen University Clinical Research Foundation of 5010 Project (2017006 to SY).

Ethics Statement: Clinical Ethics Committee of the Experimental Animal Center, Sun Yat-sen University, approval ID:2023000209.

References

1. Sung H, Ferlay J, Siegel RL, et al. Global Cancer Statistics 2020: GLOBOCAN Estimates of Incidence and Mortality Worldwide for 36 Cancers in 185 Countries. CA Cancer J Clin. 2021;71:209–49. doi: 10.3322/caac.21660

2. Ferlay J, Ervik M, Lam F, et al. Lyon, France:: International Agency for Research on Cancer; 2024. Cancer observatory: cancer today; p. 8.https://gco.iarc.who.int/today
3. WHO Cervical cancer. 2023. https://www.who.int/zh/news-room/fact-sheets/detail/cervical-cancer
4. Poddar P, Maheshwari A. Surgery for cervical cancer: consensus & controversies. Indian J Med Res. 2021;154:284–92. doi: 10.4103/ijmr.IJMR_4240_20
5. Vavassori A, Riva G, Spoto R, et al. High precision radiotherapy including intensity-modulated radiation therapy and pulsed-dose-rate brachytherapy for cervical cancer: a retrospective monoinstitutional study. J Contemp Brachytherapy. 2019;11:516–26. doi: 10.5114/jcb.2019.90478
6. Lorusso D, Petrelli F, Coinu A, et al. A systematic review comparing cisplatin and carboplatin plus paclitaxel-based chemotherapy for recurrent or metastatic cervical cancer. Gynecol Oncol. 2014;133:117–23. doi: 10.1016/j.ygyno.2014.01.042
7. Serkies K, Jassem J. Systemic therapy for cervical carcinoma - current status. Chin J Cancer Res. 2018;30:209–21. doi: 10.21147/j.issn.1000-9604.2018.02.04
8. Orbegoso C, Murali K, Banerjee S. The current status of immunotherapy for cervical cancer. Rep Pract Oncol Radiother. 2018;23:580–8. doi: 10.1016/j.rpor.2018.05.001
9. Ferrall L, Lin KY, Roden RBS, et al. Cervical Cancer Immunotherapy: Facts and Hopes. Clin Cancer Res. 2021;27:4953–73. doi: 10.1158/1078-0432.CCR-20-2833
10. Chung HC, Ros W, Delord J-P, et al. Efficacy and Safety of Pembrolizumab in Previously Treated Advanced Cervical Cancer: Results From the Phase II KEYNOTE-158 Study. J Clin Oncol. 2019;37:1470–8. doi: 10.1200/JCO.18.01265
11. Oyouni AAA. Human papillomavirus in cancer: Infection, disease transmission, and progress in vaccines. J Infect Public Health. 2023;16:626–31. doi: 10.1016/j.jiph.2023.02.014
12. Yuan Y, Cai X, Shen F, et al. HPV post-infection microenvironment and cervical cancer. Cancer Lett. 2021;497:243–54. doi: 10.1016/j.canlet.2020.10.034
13. Vari F, Arpon D, Keane C, et al. Immune evasion via PD-1/PD-L1 on NK cells and monocyte/macrophages is more prominent in Hodgkin lymphoma than DLBCL. Blood. 2018;131:1809–19. doi: 10.1182/blood-2017-07-796342
14. He X, Xu C. Immune checkpoint signaling and cancer immunotherapy. Cell Res. 2020;30:660–9. doi: 10.1038/s41422-020-0343-4
15. Chen L, Han X. Anti-PD-1/PD-L1 therapy of human cancer: past, present, and future. J Clin Invest. 2015;125:3384–91. doi: 10.1172/JCI80011
16. 20.Gainor JF, Shaw AT, Sequist LV, et al. EGFR Mutations and ALK Rearrangements Are Associated with Low Response Rates to PD-1 Pathway Blockade in Non-Small Cell Lung Cancer: A Retrospective Analysis. Clin Cancer Res. 2016;22:4585–93. doi: 10.1158/1078-0432.CCR-15-3101
17. Yi M, Zheng X, Niu M, et al. Combination strategies with PD-1/PD-L1 blockade: current advances and future directions. Mol Cancer. 2022;21:28. doi: 10.1186/s12943-021-01489-2
18. Gupta S, Kumar P, Das BC. HPV: Molecular pathways and targets. Curr Probl Cancer. 2018;42:161–74 doi: 10.1016/j.currproblcancer.2018.03.003
19. Li C, Hua K. Dissecting the Single-Cell Transcriptome Network of Immune Environment Underlying Cervical Premalignant Lesion, Cervical Cancer and Metastatic Lymph Nodes. Front Immunol. 2022;13 doi: 10.3389/fimmu.2022.897366
20. Gu M, He T, Yuan Y, et al. Single-Cell RNA Sequencing Reveals Multiple Pathways and the Tumor Microenvironment Could Lead to Chemotherapy Resistance in Cervical Cancer. Front Oncol. 2021;11:753386. doi: 10.3389/fonc.2021.753386
21. Chong Z-X, Ho W-Y, Yeap S-K, et al. Single-cell RNA sequencing in human lung cancer: Applications, challenges, and pathway towards personalized therapy. J Chin Med Assoc. 2021;84:563–76. doi: 10.1097/JCMA.0000000000000535
22. Heinrich S, Craig AJ, Ma L, et al. Understanding tumour cell heterogeneity and its implication for immunotherapy in liver cancer using single-cell

analysis. J Hepatol. 2021;74:700–15. doi: 10.1016/j.jhep.2020.11.036
23. van der Leun AM, Thommen DS, Schumacher TN. CD8+ T cell states in human cancer: insights from single-cell analysis. Nat Rev Cancer. 2020;20:218–32. doi: 10.1038/s41568-019-0235-4
24. Sanmamed MF, Chen L. A Paradigm Shift in Cancer Immunotherapy: From Enhancement to Normalization. Cell. 2018;175:313–26. doi: 10.1016/j.cell.2018.09.035
25. Scherl-Mostageer M, Sommergruber W, Abseher R, et al. Identification of a novel gene, CDCP1, overexpressed in human colorectal cancer. Oncogene. 2001;20:4402–8. doi: 10.1038/sj.onc.1204566
26. Urabe F, Kosaka N, Yamamoto Y. Metastatic prostate cancer-derived extracellular vesicles facilitate osteoclastogenesis by transferring the CDCP1 protein. J Extracell Vesicles. 2023;12:e12312. doi: 10.1002/jev2.12312
27. Alajati A, D'Ambrosio M, Troiani M, et al. CDCP1 overexpression drives prostate cancer progression and can be targeted in vivo. J Clin Invest. 2020;130:2435–50. doi: 10.1172/JCI131133
28. 32.Wright HJ, Hou J, Xu B, et al. CDCP1 drives triple-negative breast cancer metastasis through reduction of lipid-droplet abundance and stimulation of fatty acid oxidation. Proc Natl Acad Sci U S A. 2017;114:E6556–65. doi: 10.1073/pnas.1703791114
29. Dagnino S, Bodinier B, Guida F, et al. Prospective Identification of Elevated Circulating CDCP1 in Patients Years before Onset of Lung Cancer. Cancer Res. 2021;81:3738–48. doi: 10.1158/0008-5472.CAN-20-3454
30. Karachaliou N, Chaib I, Cardona AF, et al. Common Co-activation of AXL and CDCP1 in EGFR-mutation-positive Non-Small Cell Lung Cancer Associated With Poor Prognosis. EBioMedicine. 2018;29:112–27. doi: 10.1016/j.ebiom.2018.02.001
31. Harrington BS, He Y, Khan T, et al. Anti-CDCP1 immuno-conjugates for detection and inhibition of ovarian cancer. Theranostics. 2020;10:2095–114. doi: 10.7150/thno.30736.
32. Chopra S, Trepka K, Sakhamuri S, et al. Theranostic Targeting of CUB Domain-Containing Protein 1 (CDCP1) in Multiple Subtypes of Bladder Cancer. Clin Cancer Res. 2023;29:1232–42. doi: 10.1158/1078-0432.CCR-22-1973
33. Moroz A, Wang Y-H, Sharib JM, et al. Theranostic Targeting of CUB Domain Containing Protein 1 (CDCP1) in Pancreatic Cancer. Clin Cancer Res. 2020;26:3608–15. doi: 10.1158/1078-0432.CCR-20-0268
34. Lim SA, Zhou J, Martinko AJ, et al. Targeting a proteolytic neoepitope on CUB domain containing protein 1 (CDCP1) for RAS-driven cancers. J Clin Invest. 2022;132:e154604. doi: 10.1172/JCI154604
35. Liu H, Ong S-E, Badu-Nkansah K, et al. CUB-domain-containing protein 1 (CDCP1) activates Src to promote melanoma metastasis. Proc Natl Acad Sci U S A. 2011;108:1379–84. doi: 10.1073/pnas.1017228108
36. Law ME, Ferreira RB, Davis BJ, et al. CUB domain-containing protein 1 and the epidermal growth factor receptor cooperate to induce cell detachment. Breast Cancer Res. 2016;18:80. doi: 10.1186/s13058-016-0741-1
37. Uekita T, Fujii S, Miyazawa Y, et al. Oncogenic Ras/ERK signaling activates CDCP1 to promote tumor invasion and metastasis. Mol Cancer Res. 2014;12:1449–59. doi: 10.1158/1541-7786.MCR-13-0587
38. Cen Y, Zhu T, Zhang Y, et al. hsa_circ_0005358 suppresses cervical cancer metastasis by interacting with PTBP1 protein to destabilize CDCP1 mRNA. Mol Ther Nucleic Acids. 2022;27:227–40. doi: 10.1016/j.omtn.2021.11.020
39. Huang L, Chen Y, Lai S, et al. CUB Domain-Containing Protein -1 Promotes Proliferation, Migration and Invasion in Cervical Cancer Cells. Cancer Manag Res. 2020;12:3759–69. doi: 10.2147/CMAR.S240107
40. Jiang P, Gu S, Pan D, et al. Signatures of T cell dysfunction and exclusion predict cancer immunotherapy response. Nat Med. 2018;24:1550–8. doi: 10.1038/s41591-018-0136-1
41. Borjini N, Lun Y, Jang G-F, et al. CD6 triggers actomyosin cytoskeleton remodeling after binding to its receptor complex. J Leukoc Biol. 2024;115:450–62. doi: 10.1093/jleuko/qiad124
42. 47.Ogiwara Y, Nakagawa M, Nakatani F. Blocking FSTL1 boosts NK immunity in treatment of osteosarcoma. Cancer Lett. 2022;537:215690. doi: 10.1016/j.canlet.2022.215690
43. Wong S-C, Yeh C-C, Zhang X-Y, et al. Inhibition of CDCP1 by 8-isopentenylnaringenin synergizes with EGFR inhibitors in lung cancer treatment. Mol

Oncol. 2023;17:1648–65. doi: 10.1002/1878-0261.13429

44. Cai D, Li J, Liu D, et al. Tumor-expressed B7-H3 mediates the inhibition of antitumor T-cell functions in ovarian cancer insensitive to PD-1 blockade therapy. Cell Mol Immunol. 2020;17:227–36. doi: 10.1038/s41423-019-0305-2
45. Wang J, Sun J, Liu LN, et al. Siglec-15 as an immune suppressor and potential target for normalization cancer immunotherapy. Nat Med. 2019;25:656–66. doi: 10.1038/s41591-019-0374-x
46. Consuegra-Fernández M, Lin F, Fox DA, et al. Clinical and experimental evidence for targeting CD6 in immune-based disorders. Autoimmun Rev. 2018;17:493–503. doi: 10.1016/j.autrev.2017.12.004
47. Aragón-Serrano L, Carrillo-Serradell L, Planells-Romeo V, et al. CD6 and Its Interacting Partners: Newcomers to the Block of Cancer Immunotherapies. Int J Mol Sci. 2023;24:17510. doi: 10.3390/ijms242417510
48. Enyindah-Asonye G, Li Y, Ruth JH, et al. CD318 is a ligand for CD6. Proc Natl Acad Sci U S A. 2017;114:E6912–21. doi: 10.1073/pnas.1704008114
49. Xue C, Yao Q, Gu X, et al. Evolving cognition of the JAK-STAT signaling pathway: autoimmune disorders and cancer. Signal Transduct Target Ther. 2023;8:204. doi: 10.1038/s41392-023-01468-7
50. Owen KL, Brockwell NK, Parker BS. JAK-STAT Signaling: A Double-Edged Sword of Immune Regulation and Cancer Progression. Cancers (Basel) 2019;11:2002. doi: 10.3390/cancers11122002
51. Wee S, Schieven GL, Kirihara JM, et al. Tyrosine phosphorylation of CD6 by stimulation of CD3: augmentation by the CD4 and CD2 coreceptors. J Exp Med. 1993;177:219–23. doi: 10.1084/jem.177.1.219
52. Velasco-de Andrés M, Casadó-Llombart S, Català C, et al. Soluble CD5 and CD6: Lymphocytic Class I Scavenger Receptors as Immunotherapeutic Agents. Cells. 2020;9:2589. doi: 10.3390/cells9122589
53. Henriques SN, Oliveira L, Santos RF, et al. CD6-mediated inhibition of T cell activation via modulation of Ras. Cell Commun Signal. 2022;20:184. doi: 10.1186/s12964-022-00998-x
54. Gonçalves CM, Henriques SN, Santos RF, et al. CD6, a Rheostat-Type Signalosome That Tunes T Cell Activation. Front Immunol. 2018;9:2994. doi: 10.3389/fimmu.2018.02994
55. Chalmers SA, Ayilam Ramachandran R, Garcia SJ, et al. The CD6/ALCAM pathway promotes lupus nephritis via T cell–mediated responses. J Clin Invest. 2022;132:e147334. doi: 10.1172/JCI147334
56. Chalmers SA, Ayilam Ramachandran R, Garcia SJ, et al. The CD6/ALCAM pathway promotes lupus nephritis via T cell-mediated responses. J Clin Invest. 2022;132:e147334. doi: 10.1172/JCI147334.
57. Castro MAA, Oliveira MI, Nunes RJ, et al. Extracellular isoforms of CD6 generated by alternative splicing regulate targeting of CD6 to the immunological synapse. J Immunol. 2007;178:4351–61. doi: 10.4049/jimmunol.178.7.4351
58. Brunelli E, Minassi A, Appendino G, et al. 8-Prenylnaringenin, inhibits estrogen receptor-alpha mediated cell growth and induces apoptosis in MCF-7 breast cancer cells. J Steroid Biochem Mol Biol. 2007;107:140–8. doi: 10.1016/j.jsbmb.2007.04.003
59. den Boon JA, Pyeon D, Wang SS, et al. Molecular transitions from papillomavirus infection to cervical precancer and cancer: Role of stromal estrogen receptor signaling. Proc Natl Acad Sci USA. 2015;112:E3255–64. doi: 10.1073/pnas.1509322112